Cellular and Molecular Biology ™ **53**, OL1018-OL1024
DOI 10.1170/116

ISSN 1165-158X
2007 Cell. Mol. Biol.™

KINETICS OF INTRACOLLOIDAL IODINE IN THYROID OF IODINE-DEFICIENT OR EQUILIBRATED NEWBORN RATS. DIRECT IMAGING USING SECONDARY ION MASS SPECTROMETRY.

M. ELBAST[1], T.D. WU[2, 3], F. GUIRAUD-VITAUX[1], J.L. GUERQUIN-KERN[2,3], A. PETIET[1], E. HINDIE[1], C. CHAMPION[3], A. CROISY[2, 3], N. COLAS-LINHART[1]✉

[1]✉Biophysique. UFR de Médecine. Site Xavier Bichat. BP 416. 75870 Paris cedex 18. France.
Tel. 33(1) 44 85 63 09 – Fax. 33(1) 44 85 63 07 – Email : radiobioexp@aol.com
[2] Institut Curie, Laboratoire de Microscopie Ionique, Orsay 91405. France.
[3]INSERM, U759, Orsay 91405. France
[4]Physique Moléculaire et des Collisions. Institut de Physique. 1 bd Arago. 57078 Metz cedex 03. France.

Received October 1st, 2007; Accepted November 11th, 2007; Published December 30th, 2007

Abstract – The most significant impact of the Chernobyl accident is the increased incidence of thyroid cancers among children. In order to accurately estimate the radiation dose provided by radioiodines, it is important to examine how the distribution of newly incorporated iodine varies with time and if this distribution varies according to the iodine status. The kinetic distribution of intra colloidal newly organified iodine in the rat immature thyroid was recorded and analysed using the ionic nanoprobe NanoSims50™. Our observations imply that in case of radioiodine contamination, the energy deposits vary (i) with time, (ii) from one follicle to another, and (iii) from one cell to another inside the same follicle regardless the iodine status. The kinetic heterogeneity of iodine distribution must be take in account in thyroid dose evaluation.

Key words: Thyroid follicles, iodine kinetic, SIMS, radioiodines, iodine deficiency.

INTRODUCTION

The most significant consequence of the Chernobyl accident is the increased incidence of thyroid cancers in children and adolescents who were exposed to radioiodines fallout from the atmospheric release (17, 30). Since then, there has been renewed interest in radioiodine thyroid dosimetry and in the effects of radioiodines, especially in children (18, 35).

In addition to 131 iodine (^{131} I), short-live radioiodines were involved in an increase in thyroid cancers in Marshall Island inhabitants exposed to nuclear fallout (21). Despite this, short-lived radioiodine effects have not been considered in most calculations involving the after-effects of the Chernobyl accident, and thyroid cancers were mainly attributed to ^{131}I (4,22), with only a few studies (2,3,13) pointing out the possible role of short-lived radioiodines. Moreover, radioiodine radiation doses applied to the thyroid, whether they result from therapeutic measures or accidental exposure, are always based on the hypothesis of a uniformly distributed activity within the thyroid resulting in a uniform irradiation of the organ (12,23). In addition, conventional methods for radiation dose calculations implicitly assume that the radiation dose received by each cell is the same as the dose received by the entire organ. However, as early as 1956, Sinclair *et al.* showed the heterogeneity of ^{131}I incorporation within the thyroid using autoradiography (31). Recently, the distribution of ^{131}I radio-induced thyrocyte damage was shown to be heterogeneous, suggesting that iodine is not incorporated homogeneously in thyroid tissue (16). Large differences in iodine

Abbreviations: SIMS, Secondary ion mass spectrometry.

uptake in newborn rat thyroid follicles have also been observed using secondary ion mass spectrometry (SIMS microscopy) (19). Furthermore, the fallout of radioiodines from the Chernobyl accident occurred in regions of Ukraine and Belarus in which the resident's diets are considered moderately deficient in dietary iodine (28). The relation between dietary iodine status and thyroid uptake of radioiodine is well known. Nevertheless, some authors suggest that the higher risk of thyroid cancer in people with iodine deficiency is not only due to higher thyroid uptake, but also because of the greater heterogeneous distribution of iodine in the follicle and that the distribution of incorporated iodine varies with time (20).

In order to accurately estimate the radiation dose provided by radioiodines, it is important to examine how the distribution of newly incorporated iodine varies with time and if this distribution varies according to the iodine status.

The objective of this study is to describe the kinetic distribution of newly organified iodine in the immature thyroid. The kinetic profile will allow us to propose an improved dynamic model for the dosimetric evaluation of the thyroid gland.

During the study, we recorded the variations in intracolloidal iodine distribution from 1 hour to 8 days after administration of 129 iodine (^{129}I) in newborn rats under standard or low-iodine diets. The age at which the animals were contaminated was chosen to correspond to the age-range where the increase in thyroid cancers was greatest after the Chernobyl accident. Tissue analysis was performed using secondary ion mass spectrometry (SIMS), an elemental technique for the study of isotopic compositions in solid samples (11). In our work, isotopic analysis was used to discriminate between the natural ^{127}I, the isotope of the initial pool of iodine, and ^{129}I, the isotope of the newly incorporated iodine. This technique has successfully been applied to map the distribution of elements and molecules in individual cells within tissue sections or cell cultures (18). Thyroid samples were analyzed using the new ionic nanoprobe NanoSims50^{TM} (CAMECA, Paris, France). The main characteristics of this new instrument are a high lateral resolution ($\leq$ 50 nm), the ability to measure up to 5 masses (ions) in parallel in the same microvolume, a very good mass transmission at high resolutions, and direct optical observation of the sample in the ionization chamber, allowing for easy selection of areas of interest (14).

MATERIALS AND METHODS

Animals

The study was carried out on newborn Wistar rats from 4 female rats. Two dams were fed with a low-iodine diet (TD0097 Tekkad Harlan, USA) containing 25 to 50 µg of iodine per kilogram of dry food weight, for at least 3 weeks prior mating and for all the duration of the study. Two other dams were fed with a standard diet containing 2 mg of iodine per kilogram of dry food weight. After 21 to 22 days of gestation, the dams had given birth and offspring were separated into 4 groups, each litter corresponding to one of the groups: 7N, 7H, TN and TH. All the pups were prevented access to suckling from their mother.

The pups of groups 7N (pups under standard diet) and 7H (pups under low iodine diet) at 7 days old received one subcutaneous injection of 0.2 µg ^{129}I , (^{129}I-Na^{+}, NEN Life Science products, Boston MA, USA), with an activity of 1.2 Bq, in a 50 µl volume.

Pups were sacrificed by exsanguination 1, 4, 8, 24 hours, 4 and 8 days after ^{129}I-Na^{+} administration

"Age-control" newborn rats (i.e. without contamination) from the remaining litters (TN and TH) were sacrificed at 7 days, 12 days, and 15 days corresponding to the age at the sacrifice time of "contaminated" pups, to avoid contamination though suckling.

Sample preparation

Immediately after sacrifice, thyroids of control and "contaminated" pups were removed and fixed in 2.5% cacodylate-buffered glutaraldehyde, washed, dehydrated in alcohol series, and embedded in epoxy resin. This method is well suited for preserving the localization and local concentrations of iodine bound to macromolecules (9).

Serial thin sections (thickness 0.5 µm, surface about 1 mm^2) were deposited on glass slides for light microscopy, and on stainless steel disks (2 to 3 sections) for SIMS analysis. Observation of thyroid sections under light microscopy allowed a selection of region of interest prior to SIMS imaging to locate follicles with colloidal matter and a diameter of about 20 µm for ion imaging.

NanoSIMS analysis

SIMS observations were carried out on a NanoSims50^{TM} microbeam analyzer using a cesium primary beam. Separate images were recorded for the initial iodine pool (^{127}I) and the distribution of newly organified iodine (^{129}I). Topography was revealed using ^{31}P, which associates both with DNA in the cell's nucleus and phosphorylated cytoplasmic molecules, and ^{32}S, which allows the identification of the thyrocolloid.

The primary beam used had an intensity of 5 pA with a probe size (68% intensity) of about 150 nm in diameter for an analyze areas of 50 µm side (3 to 4 follicles). All of the images were recorded with a definition of 256 pixels x 256 pixels. The typical acquisition duration was 5 ms per pixel for ^{32}S^{-} and ^{127}I^{-} with respect to longer counting time of 15 ms per pixel for ^{31}P^{-} and ^{129}I^{-} species at much lower intensity. During analysis of biological specimens, polyatomic ions emitted at nearly the same mass may interfere with the species of interest. A previous study has shown that a nominal mass resolving power of 4830

(defined as M/ΔM, where M is the studied mass and ΔM the difference which separates it from the mass of an isobaric species to be distinguished) must be employed during the measurement of low intensity $^{129}I^-$ ions due to the presence of an unidentified polyatomic species (14) (Fig.1).
Images of thyroids of control newborn rats recorded using these experimental conditions are shown in fig. 2 where the detected signal at mass 129 corresponds to the random background noise of the detector.

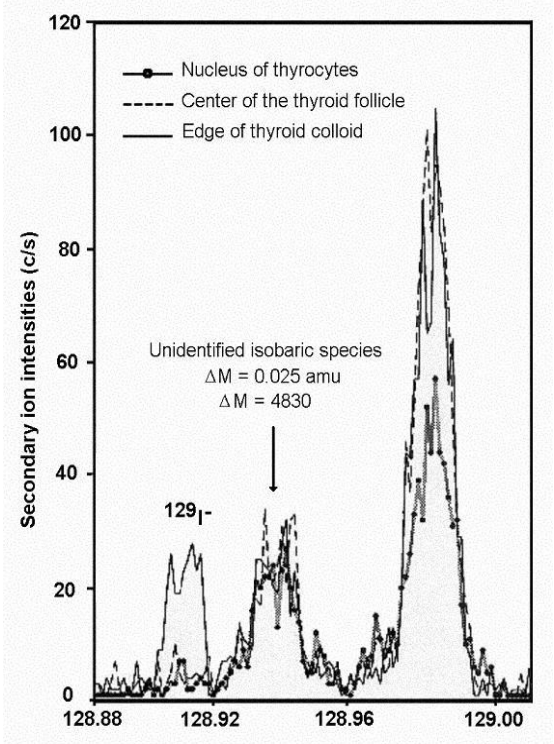

Figure 1. High resolution mass spectra recorded at mass 129 on various regions of a rat thyroid. ^{129}I is only found at the edge of the thyroid colloid. A mass resolving power of 4830 is required to distinguish between $^{129}I^-$ and a polyatomic species with nearly the same mass.

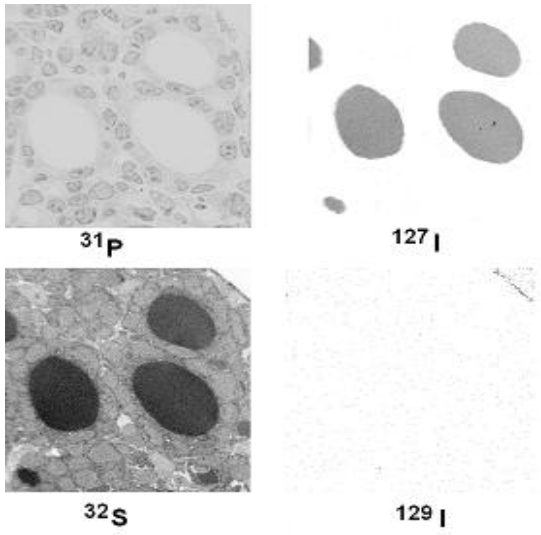

Figure 2. Ionic images of a TN newborn rat (field: 50 × 50 µm). The few scattered particles seen on the ^{129}I image are due to the detector background noise, which exhibits a random distribution. All of the images are shown with inverted grays scale (dark = high signal).

To evaluate the variation of distribution with time with acceptable statistics, large field ionic images from 60 to 120 µm were recorded. For each animal group and at each time of sacrifice, the number of follicles showing homogeneous repartition of ^{129}I and those showing heterogeneous repartition were scored. A percentage of "heterogeneity" was calculated at each time, corresponding to the number of heterogeneous follicles to the total of observed follicles.

RESULTS

At mass 127 the recorded images show that the distribution of iodine is homogeneous within the colloid, whatever the age of the animal and the iodine status. Slight inter follicular variations in the distribution of stable iodine were occasionally observed

The distribution of newly organified ^{129}I in the lumen of thyroid follicles varies with time.

In Figure 3, pseudo-colors were used to superimpose images obtained for ions $^{31}P^-$ and $^{129}I^-$. Images for ion $^{127}I^-$ were not superimposed, because they hindered the view of the different distribution profiles of newly incorporated iodine. Ionic images obtained at early times (Figs. 3A, 3B,) show that ^{129}I is found at the periphery of the colloid as a ring in the 7N pups as well as in the 7H pups. Nevertheless, some follicles with a homogeneous distribution of ^{129}I were observed, mostly in the 7H group. At eight hours after administration (Fig. 3C), the distribution of ^{129}I is homogeneous within most follicles but can still appear slightly heterogeneous in some follicles particularly in 7N group.

At days 1, 4, and 8, all analyzed follicles displayed a homogeneous distribution of ^{129}I (Fig. 3D, 3E, 3F).

It is noteworthy that this iodine distribution is very heterogeneous four hours after administration. ^{129}I is seen concentrated at the periphery of the colloid, close to the thyroid cells (Fig. 4). However, even at this early stage, some follicles display a homogeneous distribution of ^{129}I.

Different patterns of newly incorporated iodine distribution have been observed: homogeneous distribution within the colloid or as a ring distribution. The number of follicles showing homogeneous repartition of ^{129}I and those showing heterogeneous repartition were scored. In Fig. 5 a percentage of "heterogeneity" calculated at each time is presented. There is a slight influence of the iodine status. "Ring" distribution are only observed on ionic images recorded before 24 hours. In 7N pups a high

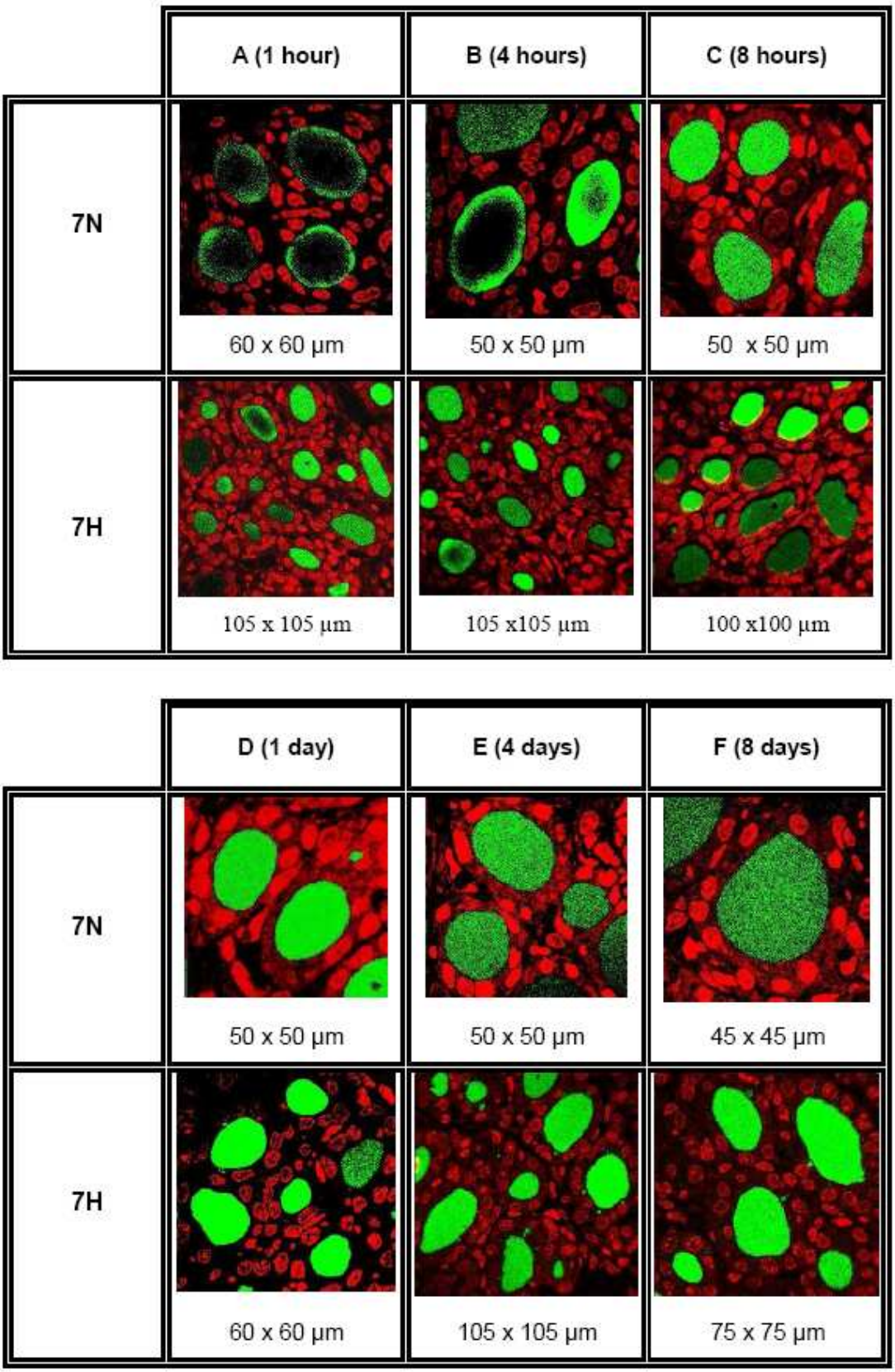

Figure 3. Kinetic of intrafollicular iodine. Pseudo-colors were used to superimpose ionic images obtained for ions $^{31}P^-$ (red) and $^{129}I^-$(green) with : A, images obtained 1 hour after ^{129}I administration, B, 4 hours, C, 8 hours, D, 1 day, E, 4 days and F, 8 days after ^{129}I administration. Dimensions of the analysis field are given under the ionic images.

percentage of heterogeneous follicles (92, 100 %) is noted until 4 hours after "contamination". In iodine deficient pups, the percentages are markedly lower, about 20 %. From 8 hours to 8 days after "contamination", only homogeneous follicles are observed in all thyroid samples.

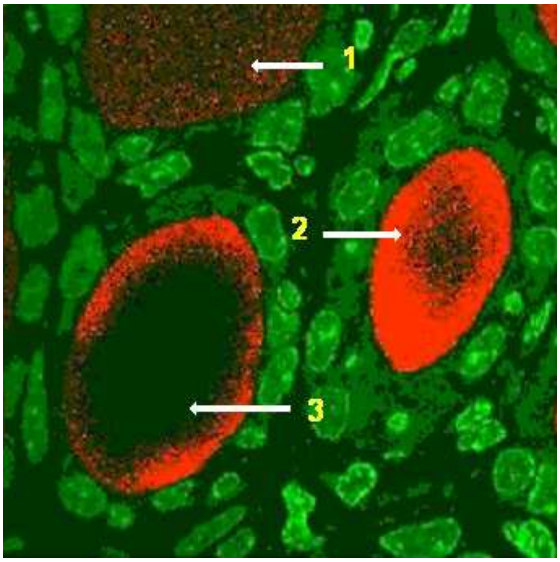

Figure 4. Digitized image in pseudo-colors with superimposition of ^{31}P (green), and ^{129}I (red) of a group 7N rat's thyroid follicle, 4 hours after "contamination" showing the different patterns of ^{129}I distribution. Arrow 1: homogeneous follicular distribution. Arrow 2 and 3: distribution as a ring. Note: the distribution within the ring is itself highly heterogeneous.

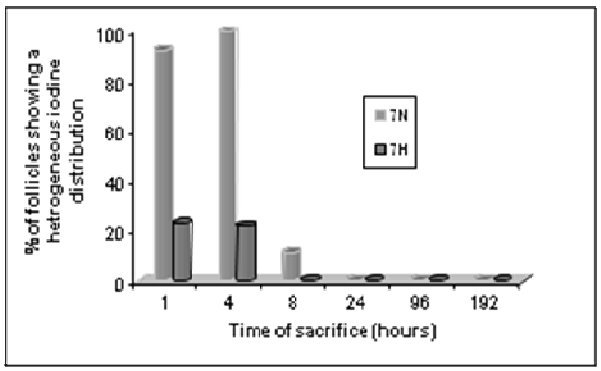

Figure 5. Percentage of heterogeneous follicles as a function of contamination time. The percentage of follicles with a heterogeneous distribution profile is higher in 7N group than in 7H group. It seems that iodine deficiency accelerates the intra follicular incorporation of iodine.

DISCUSSION

Iodine distribution in thyroid gland follicles is usually evaluated indirectly by autoradiography (1, 27) or the expression of proteins involved in the iodine pathways such as the sodium/iodide symporter (NIS, responsible for active iodide uptake from the bloodstream to the thyrocyte) or pendrin (7). The main advantage of SIMS microscopy is the ability to make direct observations of the distribution of any element occurring at the surface of a sample, with no need for specific labeling with a fluorescent or radioactive probe.

SIMS microscopy is a powerful technique for studying the distribution of elements in biological tissues at the cellular level. Although having provided important information on stable and radioactive iodine distribution within the thyroid in normal and disturbed circumstances (9,10,25), this technique has been considered a marginal method in biology because of its poor lateral resolution (1 to 0.5 µm), and the insufficient mass separation power of the early instruments (8). Indeed, the main difficulty with SIMS microscopy is signal specificity which is highly dependent on mass resolution: the complexity of the organic matrix leads to the emission of a large number of ions which can interfere with the study element. The latest high-resolution dynamic SIMS device (NanoSims50^{TM}) that we used in our work has both a very good transmission at high mass resolutions, and a high lateral resolution ($\leq$ 50 nm). Recently, the ultra-structural localization of ^{127}I-benzamide uptake in melanin grains within melanocytes was performed using the NanoSims50^{TM} device (15).

The animal model in our study was set up to mimic the conditions of contamination by radioiodine by Chernobyl fallout: young age and mild iodine deficiency.

No increase of thyroid volume was observed in the iodine deficient pups. All changes were manifested as differences in histological morphology of the thyroid. No difference was found between the follicular diameter of iodine deficient pups and normal pups, but significant differences were found for colloid diameters and cell heights: the colloid was rarefied at the expense of cellular height in the iodine deficient pups.

The age of administration of radiotracer was chosen to correspond to the typical age of contamination of children who have developed thyroid papillary carcinomas, years after the Chernobyl accident (32)

The use of ^{129}I permits us to discriminate newly organified iodine (mass 129) to the initial pool of ^{127}I stable iodine (mass 127) using SIMS microscopy. The ^{129}I radioisotope has a very long

physical half-life (1.7×10^7 years), which allows us to perform time-consuming sample preparation without signal transformation, and to avoid radiobiological effects on the thyroid of the newborn rats (administered activity: 1.2 Bq). Moreover, no evidence of cell necrosis was seen in the thyroid sections. The administered amount of 200 ng ^{129}I per pup was based on a compromise between the quantity incorporated by the thyroid (10% of the injected mass ie 20 ng for normal pups and 20 % ie 40 ng for iodine deficient pups) in order to provide correct acquisition time of ionic images, and avoidance of the Wolff-Chaikoff effect on the thyroid cells. (The Wolff-Chaikoff effect is the inhibition of organic binding of iodine in the thyroid by an excess of iodine) (24,33)

Our results clearly demonstrate that, whatever the iodine status, distribution of newly organified iodine is heterogeneous within and between follicles newborn rat thyroids and that the distribution varies as a function of time. These results are in agreement with those observed previously by Hindié et al (19). Only slight influence of iodine status has been observed: lower number and fast disappearance of heterogeneous follicles in 7H pups. This suggests that iodine deficiency should be an element of acceleration of iodine intrafollicular incorporation according to Desmarais et al. (6), who concluded that previous levels of iodine intake strongly influence the rate of iodine incorporation. Furthermore, we noted a high degree of heterogeneity in the distribution of ^{129}I within the ring-like image, which could possibly be related to a functional heterogeneity of thyrocytes within the same follicle as also suggested by the heterogeneity of the expression of NIS (26).

Importantly, our observations imply that in case of radioiodine contamination, the energy deposits vary (i) with time, (ii) from one follicle to another, and (iii) from one thyrocyte to another inside the same follicle. Early after contamination, the ring-like distribution of iodine within the colloidal matter may result in higher concentrations of radioactive iodine close to the thyroid cells; thus, short-lived iodine will have a high proportion of decay events concentrated close to the thyroid cells. In addition, it is well known that thyroidal uptake of radioiodine is inversely proportional to the quantity of iodine already present in the gland and in case of radioiodine contamination, thyroid cells of a iodine deficient gland will be more irradiated than those in a iodine equilibrated gland (29).
The kinetics of iodine distribution in the follicle allow us to elaborate a model to calculate the contribution of short-lived radioiodines, to accurately calculate the thyroid cellular doses. We are working in this direction. Dose deposits in biological matter can be described using a detailed Monte Carlo model based on theoretical cross-section calculations (5). A combination of both of the above models would allows us to follow, step-by-step at the nanometric scale, the primary β^- particles produced by the entire spectrum of iodine decay, as well as the secondary β^- particles created along the trajectory of the primary particles.

In conclusion, these observations suggest that in case of contamination by a radioiodine combination, most of the dose will be delivered during the maximal intrafollicular heterogeneity stage, regardless of iodine status, and thus the kinetic heterogeneity of iodine distribution must be take in account in thyroid dose evaluation.

Several studies using the NanoSims50^{TM} are currently under way in our laboratory in order to determine the precise role of age at contamination on follicular iodine distribution. Indeed, Faggiano et al. (7) have found an age-related variability in the thyroid's morphofunctional status and suggested that the distribution of iodine in the follicles could vary according to age. Nonetheless, to date, the decrease with age in thyroid radio-sensitivity is not entirely understood (34).

Acknowledgments - This study was supported by grant RB 2005- 09 from Electricité de France. The author's thank Dr Eric Broneer and Pr Michael Stabin for editing manuscript and helpful comments.

REFERENCES

1. Ahuja, S., Schiller, S. and Ernst H., An autoradiographic study of postoperatively labeled thyroid tissue and iodine storage. *Eur J Nucl Med.* 1991, 18: 791-795.
2. Balanov, M., Kaidanovski, G., Zvonova, I., Kovtun, A., Bouville, A., Luckyanov, N. and Voillecque, P., Contributions of short-lived radioiodine to thyroid doses received by evacuees from the Chernobyl area estimated using early in vivo activity measurements. *Radiat Prot Dos*. 2003, 105: 593-599.
3. Bleuer, J.P., Averkin, Y.I. and Abelin, T., Chernobyl-related thyroid cancer: what evidence for short-lived iodines? *Environ Health Perspect.* 1997, 105: 1483-1486.
4. Cardis, E., Kesiniene, A., Ivanov, V., Malakhoova, I., Shihabata, Y., Krouch, V., *et al*. Risk of thyroid cancer after exposure to ^{131}I in childhood. *J Natl Cancer Inst*. 2005, 97: 724-32.
5. Champion, C., Theoretical cross sections for electron collisions in water: structure of electron tracks. *Phys Med*

Biol. 2003, 48: 2147-2168.
6. Desmarais, A. and Laham, Q.N., The relation between the staining properties of the thyroidal colloid and its iodine content. *Can J Biochem.* 1962, 40: 227-236.
7. Faggiano, A., Coulot J., Bellon, N., Talbot, M., Caillou, B., Ricard, M., Bidart, J.L. and Schlumberger, M., Age-dependent variation of follicular size and expression of iodine transporters in human thyroid tissue. *J Nucl Med*. 2004, 45: 232-237.
8. Fourré, C., Petiet, A. and Colas-Linhart, N., Mutual contribution by "track" microradioautography method (MRA) and secondary ion mass spectrometry (SIMS) microscopy: Prospects in technetium dosimetry at the cellular level. *Cell. Mol. Biol.* 1996, 42: 385-393.
9. Fragu, P., Briançon, C., Halpern, S. and Larras-Regard, E., Changes in iodine mapping in rat thyroid during the course of iodine deficiency: imaging and relative quantification by analytical ion spectrometry. *Biol Cell*. 1988, 65: 145-155.
10. Fragu, P., Halpern, S., Briançon, C., Olivo, J.C. and Kahn, E., Imagerie microscopique fonctionnelle de la glande thyroïde. *Path Biol.* 1991, 39: 1029-1037.
11. Fragu, P., Briançon, C., Fourré, C., Clerc, J., Casiraghi, O., Jeusset, J., Omri, F. and Halpern, S., SIMS microscopy in the biomedical field. *Biol Cell*. 1992, 74: 5-18.
12. Goulko, G.M., Chumak, V., Chepurny, N., Henrichs, K., Jacob, P., Kairo, I.A., Likhtarev, I., Repin, V., Sobolev, B.G. and Voigt G., Estimation of 131I thyroid doses from the evacuees from Pripyat. *Radiat Environ Biophys.* 1996, 35: 81-87.
13. Gavrilin, Y.I., Khrouch, V.T., Shinkarev, S.M., Drozdovitch, V.V., Minenko, V.F., Shemiakina, E., Ulanovsky, A., Bouville, A., Anspaugh, L., Voillequé, P. A. and Luckyanov N., Individual thyroid dose estimation for a case-control study of Chernobyl related thyroid cancer among children of Belarus – Part 1: ^{131}I, short-lived radioiodines (^{132}I, ^{133}I, ^{135}I) and short-lived radiotelluriums (^{131m}Te and v ^{132}Te). *Health Phys.* 2004, 86: 565-585.
14. Guerquin-Kern, J.L., Wu, T.D., Quintana, C. and Croisy, A., Progress in analytical imaging of the cell by dynamic secondary ion mass spectrometry. *Biochim Biophys Acta*. 2005, 1724: 228-238.
15. Guerquin-Kern, J.L., Hillion, J.C., Madelmont, J.C., Labarre, P., Papon, J. and Croisy, A., Ultra-structural cell distribution of the melanoma marker iodobenzamide: improved potentiality of SIMS imaging in life sciences. *Biomed. Eng. Online*. 2004, 3: 1-7.
16. Guiraud-Vitaux, F., Feldmann, G., Vadrot, N., Charles-Gupta, S., Durand-Schneider, A.M., Colas-Linhart, N. and Petiet A., Early ultrastructural injuries in the thyroid of the normal rat radioinduced by diagnostic and or therapeutic amounts of iodine-131. *Cell. Mol. Biol.* 2001, 47: 495-502.
17. Heidenreich, W.F., Kenigsberg, J., Jacob, P., Buglova, E., Goulko, G., Pareztke, H.G., Demidchik, E.D. and Golovneva A., Time trends of thyroid cancer incidence in Belarus after the Chernobyl accident. *Radiat Res*. 1999, 151: 617-625.
18. Heidereich,W.F., Kayro,I., Chepurny, M., Jacob,P., Spak, V., Goulko, G.M. and Paretzke, H.G., Age- and sex-specificity relative thyroid radiation exposure to ^{131}I in Ukraine after the Chernobyl accident. Health Phys. 2001, 80: 242-250.
19. Hindié, E., Petiet, A., Bourahla, K., Colas-Linhart, N., Slodzian G., Dennebouy, R. and and Galle, P., Microscopic distribution of iodine radioisotopes in the thyroid of the iodine deficient newborn rat: insight concerning the Chernobyl accident. *Cell. Mol. Biol*. 2001, 47: 403-410.
20. Hindié, E., Leenhart, L., Vitaux, F., Colas-Linhart, N., Grosclaude, P., Galle, P., Aurengo, A. and Bok, B., Non-medical exposure to radioiodine and thyroid cancer. *Eur J Nucl Med*. 2002, 29: S497-S512.
21. Howard, J.E., Vaswani, A. and Heotis, P., Thyroid disease among the Rongelap and Utirik population – An update. *Health Phys*. 1997, 73: 190-198.
22. Jacob, P., Kenigsberg, Y., Zvonova, I., Goulko, G., Buglova, E., Heidenreich W.F., Golovneva A., Bratilova, A.A., Drozdovitch, V., Kruk, J., Pochtennaja, G.T., Balanov, M., Demidchik, E.P. and Paretzke, H.G., Childhood exposure due to the Chernobyl accident and thyroid cancer risk in contaminated areas of Belarus and Russia. *Brit J Can*. 1999, 80: 1461-1469.
23. Loevinger, R. and Berman, M. A., revised schema for calculating the absorbed dose from biological distributed radionuclides. *MIRD Pamphlet no. 1*, revised. New York: The Society of Nuclear Medicine.
24. McCoy, R.H., Dietary requirement of the rat. In: *The rat in laboratory investigation*, Farris, E.J. and Griffith, J.Q. (Eds)., J.B. Lippincott Company, London, 1942, pp 68-103.
25. Mestdagh, C., Many, M.C., Halpern, S., Briançon, C., Fragu, P. and Denef, J.F., Correlated autoradiography and ion-microscopy study of the role of iodine in the formation of "cold" follicles in young and old mice. *Cell Tissue Res*. 1990, 260: 409-457.
26. Mian, C., Lacroix, L., Alzieu, L., Nocera, M., Talbot, M., Bidart, J.M., Schumberger, M. and Caillou, B., Sodium iodide symporter and pendrin expression in human thyroid tissues. *Thyroid*. 2001, 11: 825-830.
27. Nadler, N.J., Leblond, C.P. and Bogoroch, B., The rate of iodine metabolism by the thyroid follicle as function of its size. *Endocrinology*. 1954, 52: 154-172.
28. Robbins, J., Dunn, J.T., Bouville, A., Kravchenko, V., Lubin, J., Petrenko, S., Sullivan, K., VanMiddesworth, L. and Wolff, J., Iodine nutrition and the risk from radioactive iodine. A workshop report in the Chernobyl long-term follow-up study. *Thyroid*. 2001, 11: 487-491.
29. Sehestedt, T., Knudsen, N., Perrild, H. and Johansen, C., Iodine intake incidence of thyroid cancer in Denmark. *Clin.Endocrinol*. 2006, 65: 229-233.
30. Shibata, Y., Yamashita, S., Masyakin, W.B., Panasyuk, G.D. and Nagataki, S., 15 years after Tchernobyl: new evidence of thyroid cancer. *Lancet*. 2001, 358: 1965-1966.
31. Sinclair, W.K., Abbatt, J.D., Farran, H.E., Harriss, E.B. and Lamerton, L.F., A quantitative autoradiographic study of radioiodine distribution and dosage in human thyroid gland. *Brit J Radiol.* 1956, 29, 337: 36-41.
32. UNSCEAR 2000 Report. Sources and effects of ionising radiation. In: *Vol. II. Effects of the Chernobyl accident*, New York, United Nations, 2000.
33. Wemeau, J.L., Hypothyroidism related to excess iodine. *Presse Med*. 2002, 31: 1670-1675.
34. Williams, D., Cancer after nuclear fallout: lessons from the Chernobyl accident. *Nature Rev*. 2002, 2: 546-549.
35. Zanzonico, B., Age-dependent thyroid absorbed doses for radiobiologically significant radioisotopes of iodine. *Health Phys.* 2000, 78: 60-67.